

# Inclusive $b\bar{b}$ production in ATLAS

A. Ruiz Martínez on behalf of the ATLAS Collaboration

*Iowa State University, Dpt. of Physics and Astronomy, 12 Physics Hall, Ames, IA 50011-3160, USA*

**Abstract.** The QCD production of high- $p_T$   $B$ -hadrons is an important process as a probe of perturbative QCD. High- $p_T$   $B$ -hadrons also form a significant background to many new physics channels at the LHC. Measurements of the inclusive differential  $b$ -jet cross section, where  $b$ -jets are those containing a  $B$ -hadron, are presented. The results are compared to calculations of the  $B$  cross-section based on Monte Carlos and on higher order QCD.

**Keywords:** CERN LHC, ATLAS, inclusive  $b$ -jet cross section,  $b\bar{b}$  dijet cross section, QCD

**PACS:** 12.38.Qk, 13.87.-a, 14.65.Fy

## INTRODUCTION

The measurement of the  $b$ -quark production at 7 TeV proton-proton collisions in the Large Hadron Collider (LHC) provides an important test of perturbative quantum chromodynamics (QCD) and is the first step in the understanding of other processes, such as  $W$  or  $Z$  boson production in association with  $b$ -jets, which are backgrounds in new physics searches. The first measurements of the  $b$ -jet and  $b\bar{b}$  dijet cross sections in the ATLAS detector using  $pp$  collision data acquired during 2010 are discussed here. Using secondary vertex tagging the inclusive  $b$ -jet and  $b\bar{b}$  dijet cross sections are measured with  $3.0 \text{ pb}^{-1}$  of data [1]. The inclusive  $b$ -jet cross section is also measured using the  $p_T^{\text{rel}}$  method with  $4.8 \text{ pb}^{-1}$  of data [2]. Both measurements are compared to the Monte Carlo (MC) predictions.

A detailed description of the ATLAS detector and its components can be found in Ref. [3]. The ATLAS Inner Detector consists of a silicon pixel detector (Pixel), a silicon microstrip detector (SCT) and a transition radiation tracker (TRT), surrounded by a 2 Tesla solenoid magnet. It covers the pseudorapidity range  $|\eta| < 2.5$  and has full coverage in  $\phi$ . The electromagnetic calorimeter is made of liquid-argon (LAr) as active material and lead as passive material, which has an excellent energy and position resolution and covers the pseudorapidity range  $|\eta| < 3.2$ . The hadronic calorimetry in the range  $|\eta| < 1.7$  is provided by a scintillator-tile sampling calorimeter, which is divided into a long barrel ( $|\eta| < 1.0$ ) and two extended barrels, one on each side of the central barrel ( $0.8 < |\eta| < 1.7$ ). In the end-caps ( $|\eta| > 1.5$ ), LAr hadronic calorimeters match the outer  $\eta$  limits of the end-cap electromagnetic calorimeters. The muon spectrometer consists of three superconducting toroids and a system of precision tracking chambers up to  $|\eta| < 2.7$ . ATLAS has a three-level trigger system: the Level-1, which is based on hardware, and the Level-2 and Event Filter, which are based on software.

## MEASUREMENT USING SECONDARY VERTEX TAGGING

The first measurement relies on a secondary vertex tagging algorithm to identify the  $b$ -jets. In this case the double differential inclusive  $b$ -jet cross section is measured as a function of the jet  $p_T$  and rapidity ( $y$ ) in the  $20 < p_T < 260$  GeV range. The single differential  $b\bar{b}$  dijet cross section is measured as a function of the dijet mass in the  $110 < m_{b\bar{b}} < 670$  GeV range, requiring  $p_T > 40$  GeV for the two leading jets.

Jets are built from calorimeter clusters using the anti- $k_r$  jet algorithm [4] with clustering parameter  $R = 0.4$  and are required to have rapidity  $|y| < 2.1$  to be fully contained within the acceptance of the ATLAS tracking detectors. Level-1 jet triggers are used in the analysis except for the jets with  $20 < p_T < 40$  GeV in the inclusive  $b$ -jet cross section analysis where minimum bias trigger scintillators are used. The overall trigger efficiency is above 98% for all the  $p_T$  ranges studied.

Taking advantage of the long lifetime of  $b$ -hadrons ( $\sim 1.5$  ps), which leads to a few millimeters flight path and a secondary decay vertex, the SV0 algorithm [5] has been used to reconstruct the displaced secondary vertex. The output of the algorithm is the decay length significance ( $L/\sigma_L$ ) and the selected operating point is set at 5.72 which leads to a 50% efficiency on  $t\bar{t}$  events.

For the inclusive  $b$ -jet cross section analysis, the  $b$ -tagging efficiency is determined from data using the  $p_T^{\text{rel}}$  method explained below and it is consistent with the Monte Carlo expectation within 10-15%. The fraction of  $b$ -jets in the final sample is determined by a binned likelihood fit to the secondary vertex mass distribution using MC-derived templates for the  $b$ -,  $c$ - and light-jets.

For the  $b\bar{b}$  dijet cross section analysis, the  $b$ -tagging efficiency is obtained directly from Monte Carlo. The fraction of  $b$ -jets is obtained from template fits to the distribution of the sum of the two secondary vertex masses, with templates to describe the signal (two  $b$ -jets) and the background (jet pair with at least one  $c$ - or light-jet).

A bin-by-bin correction is used to obtain the number of  $b$ -jets at the particle level. This procedure addresses the bin migrations and any remaining inefficiencies or detector effects. The bin-by-bin correction factors are obtained using Pythia [6] samples. The main systematic uncertainties affecting the analyses are the  $b$ -jet energy scale,  $b$ -tagging efficiency and template fit uncertainties, leading to an overall uncertainty of 30-40% in the inclusive  $b$ -jet cross section and a 40-60% in the  $b\bar{b}$  dijet cross section.

Figures 1 and 2 show the results for the inclusive  $b$ -jet cross section and the  $b\bar{b}$  dijet cross section respectively. Results are compared to the leading-order predictions by Pythia and the next-to-leading order (NLO) predictions derived with POWHEG [7] and interfaced to Pythia to perform the parton showering. Broad agreement between data and the MC predictions is observed within the experimental and theoretical uncertainties.

## MEASUREMENT USING THE $p_T^{\text{rel}}$ METHOD

An independent measurement of the  $b$ -jet cross section has been performed using a sample of jets containing muons. This sample was selected with a muon-plus-jet trigger which requires a reconstructed jet with  $p_T > 5$  GeV matched to a reconstructed muon with  $p_T > 4$  GeV. A jet energy correction obtained from Monte Carlo accounts for

the muon and neutrino energy. The trigger efficiency is estimated from data while the remaining efficiencies (reconstruction, selection, acceptance) are obtained from Monte Carlo.

The  $p_T^{\text{rel}}$  method is used to obtain the fraction of  $b$ -jets. The distribution of the momentum of the muon relative to the jet axis ( $p_T^{\text{rel}} = p_\mu \sin \theta$ , where  $\theta$  is the angle between the muon momentum and the direction of the associated jet) is fitted using templates derived from MC for  $b$ - and  $c$ -jets and templates extracted from data for light-jets [2].

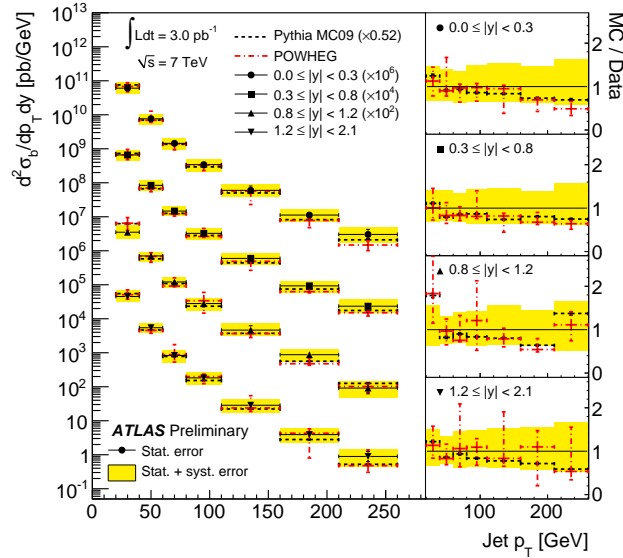


**FIGURE 1.** Inclusive double-differential  $b$ -jet cross section as a function of  $p_T$  for different rapidity regions (left) and ratio between data and Monte Carlo predictions (right). The results are compared to the Monte Carlo predictions of Pythia and POWHEG. Note that the Pythia results have been rescaled by a factor of 0.52.

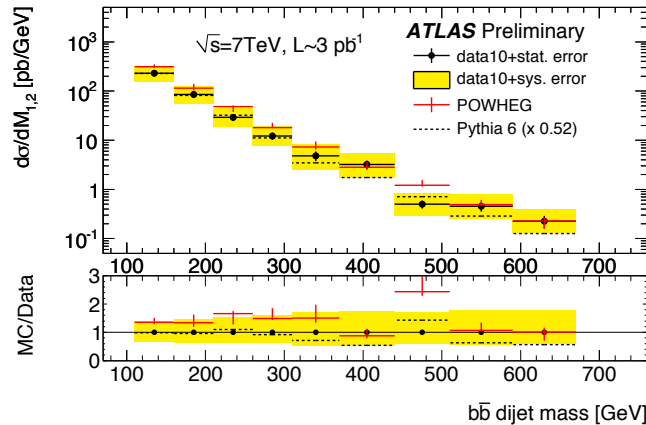


**FIGURE 2.**  $b\bar{b}$  dijet cross section as a function of the dijet invariant mass for  $|y| < 2.1$ . The results are compared to the Monte Carlo predictions of Pythia and POWHEG. Note that the Pythia results have been rescaled by a factor of 0.52.

Figure 3 shows the  $b$ -jet cross section as a function of  $p_T$  after bin-by-bin corrections and evaluation of systematics. Results are consistent with the POWHEG predictions and with the experimental results from the secondary vertex method explained above.

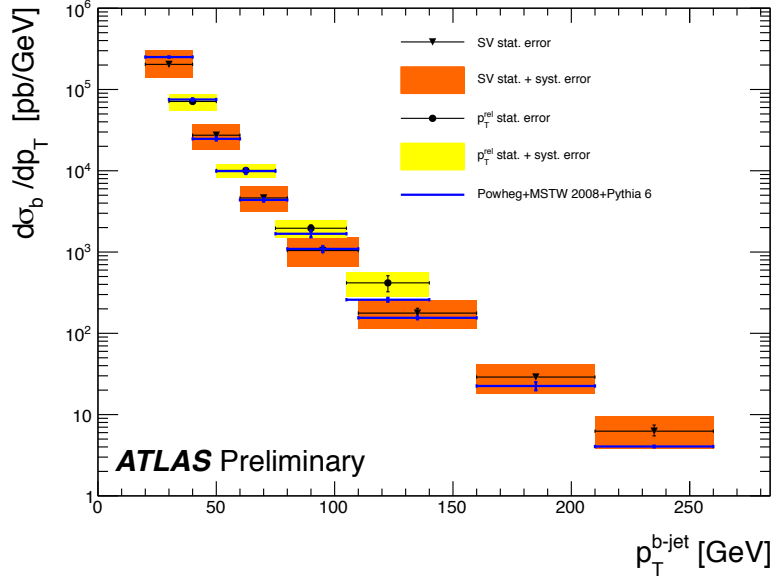


**FIGURE 3.** Comparison of  $b$ -jet differential cross section as a function of the  $p_T$  for  $|y| < 2.1$  obtained using secondary vertex tagging and with the  $p_T^{\text{rel}}$  method. The two measurements are compared to NLO predictions from POWHEG, the parton density function MSTW 2008 and Pythia 6. For the theoretical prediction, only the statistical errors are shown.

## CONCLUSIONS

The first results on the production of single jets and jet pairs from  $b$ -quarks at 7 TeV proton-proton collisions in ATLAS have been presented. Measurements based on secondary vertex tagging using  $3.0 \text{ pb}^{-1}$  of data and on the  $p_T^{\text{rel}}$  method with  $4.8 \text{ pb}^{-1}$  of data have been discussed. Both measurements are dominated by systematics and their results are in broad agreement with the NLO QCD predictions from POWHEG.

## REFERENCES

1. ATLAS Collaboration, Measurement of the inclusive and dijet cross section of  $b$ -jets in  $pp$  collisions at  $\sqrt{s} = 7 \text{ TeV}$  with the ATLAS detector, ATLAS-CONF-2011-056 (2011).
2. ATLAS Collaboration, Measurement of the  $b$ -jet production cross section using muons in jets with ATLAS in  $pp$  Collisions at  $\sqrt{s} = 7 \text{ TeV}$ , ATLAS-CONF-2011-057 (2011).
3. G. Aad, et al., *JINST* **3**, S08003 (2008).
4. M. Cacciari, G. Salam, and G. Soyez, *JHEP* **0804**, 063 (2008), arXiv:0802.1189.
5. Performance of the ATLAS Secondary Vertex  $b$ -tagging Algorithm in 7 TeV Collision Data, ATLAS-CONF-2010-042 (2010).
6. T. Sjostrand, S. Mrenna, and P. Skands, *JHEP* **05**, 026 (2006), hep-ph/0603175.
7. S. Alioli, K. Hamilton, P. Nason, C. Oleari, and E. Re, *JHEP* **04**, 081 (2011), 1012.3380.